

Electronic Supplementary Information

A Pt/SnO₂/rGO Interface more Capable of Converting Ethanol to CO₂ in Ethanol Electro-oxidation: A detailed experimental/DFT study

Peiwen Xu^{a,‡}, Shafei Zhao^{a,‡}, Tingting Wang^a, Weijie Ji^{a,*}, Zhaoxu Chen^{a,*}, and Chak-Tong Au^b

^a Key Laboratory of Mesoscopic Chemistry, MOE, School of Chemistry and Chemical

Engineering, Nanjing University, Nanjing 210023, China, jiwj@nju.edu.cn, zxchen@nju.edu.cn

^b Department of Chemistry, Hong Kong Baptist University, Hong Kong

[‡]These two authors contributed equally to this work.

Chemicals and Reagents. Tin (IV) chloride pentahydrate ($\geq 99.0\%$, $\text{SnCl}_4 \cdot 5\text{H}_2\text{O}$), anhydrous ethanol (99.7% , $\text{C}_2\text{H}_5\text{OH}$), aqueous tetramethylammonium hydroxide (25 wt.%, TMAH), ethylene glycol ($\geq 99.5\%$, EG), potassium permanganate (KMnO_4), hydrogen peroxide (30%, H_2O_2), chloric acid (HCl) and sulfuric acid (H_2SO_4) were purchased from Sinopharm Chemical Reagent Company Limited (Shanghai). Phosphoric acid (85%, H_3PO_4), chloroplatinic acid hexahydrate ($\text{Pt} \geq 37.5\%$, $\text{H}_2\text{PtCl}_6 \cdot 6\text{H}_2\text{O}$), polyvinyl pyrrolidone ($\text{MW} = 58000$, PVP), ascorbic acid (AA), natural graphite flakes were purchased from Sigma-Aldrich. Commercial Pt/C (20 wt.%, ETEK) was obtained from Johnson Matthey (JM).

Synthesis of SnO_2 rhombic dodecahedra (r.d- SnO_2). A tetramethylammonium hydroxide solution [$w(\text{H}_2\text{O}) : w(\text{TMAH } 25 \text{ wt.}\%) = 62.6 : 17.5$] was added dropwise to an aqueous solution of $\text{SnCl}_4 \cdot 5\text{H}_2\text{O}$ (1.4024 g, 4.00 mmol) of 12 ml by means of a constant pressure drop funnel. The mixture was continuously stirred for 6 h and then divided into two parts, transferred to a Teflon-lined autoclave (50 mL), and kept at 200°C for 12 h. The precipitate was collected via centrifugation and washed repeatedly with deionized water, dried at 80°C for 12 h and calcined in air at 400°C for 3 h.

Synthesis of SnO_2 octahedra (o- SnO_2) with the (111) facets. 1.4024 g $\text{SnCl}_4 \cdot 5\text{H}_2\text{O}$ was dissolved in a mixture of H_2O and ETOH ($v/v = 12/13$) of 25 ml under ultrasonic treatment. A tetramethylammonium hydroxide (TMAH) solution [$w(\text{H}_2\text{O}) : w(\text{TMAH } 25 \text{ wt.}\%) = 40 : 30.65$] was added dropwise into the aforementioned solution, and the resulting solution was continuously stirred for 12 h, and then divided into two parts, transferred to a Teflon-lined autoclave (50 mL), and kept at 200°C for 12 h. The following steps were the same as those employed in synthesis of r.d- SnO_2 .

Synthesis of SnO₂ octahedra enclosed by the (221) facets. SnCl₄·5H₂O of 1 mmol was dissolved in a solution containing 5 mL deionized water and 5 mL ethanol under ultrasonic treatment. Then PVP (0.315 g, MW=58000) was dissolved in a solution containing 5 mL deionized water and 5 mL ethanol. After that, the PVP solution and HCl (1.5 mL) were added to the mixed solution containing SnCl₄ and PVP under ultrasonic treatment. After being stirred for 3 h, the resulting solution was transferred to a Teflon-lined autoclave (50 mL) and kept at 200°C for 12 h. The precipitate was collected via centrifugation and washed repeatedly with deionized water, dried at 80 °C for 12 h.

Synthesis of SnO₂ rod-clusters (r.c-SnO₂). SnCl₄·5H₂O of 1.050 g and Na₂SO₄·5H₂O of 0.67g were dissolved in a mixture of H₂O (20 ml) and ETOH (20 ml) in a conical flask. NaOH of 1.280 g was dissolved in an ethanol-water solution of 60 ml [$v(\text{H}_2\text{O}): v(\text{ETOH}) = 1:1$]. The resulting solution was added dropwise to the conical flask, and the mixture was continuously stirred for 4 h. The mixture was divided into two parts, transferred into a Teflonlined autoclave (50 mL), and subjected to a hydrothermal treatment at 200 °C for 16 h. After the autoclave was cooled down to room temperature (RT), the precipitate was collected via centrifugation and washed repeatedly with 5 wt.% ammonia solution and distilled water. The following steps were the same as those employed in the synthesis of r.d-SnO₂.

Preparation of Pt/SnO₂ composites. The mixture of SnO₂ (50 mg) in ethylene glycol (EG, 2.5 mL) was ultrasonically dispersed and then preheated at 120 °C for 10 min. After that a polyvinylpyrrolidone (PVP, MW = 55 000) solution of totally 3 mL (1.125 M, 94 μL each time) and a H₂PtCl₆·6H₂O solution of totally 1.5 mL (17 mM, 47 μL each time) were added into the SnO₂-EG suspension under vigorous stirring within a period of 16 min. The resulting mixture

was kept at 120 °C for additional 10 min and then cooled down to RT. The obtained product was collected by centrifugation and washed thoroughly with water and ethanol several times. The samples were further dried overnight at 323 K under vacuum.

Preparation of GO suspension^[1] and /Pt/SnO₂/rGO composites. Graphene oxide (GO) was prepared by the modified Hummers' method.^[2] In a typical procedure, the GO and Pt/SnO₂ (10 mg) were dispersed in 30 mL water and sonicated for 1 h. Subsequently, 2 mL of AA (10 mg mL⁻¹) was added to the above suspension, and sonicated at 60 °C for another 1 h. The obtained black suspension was washed with water several times and dried under vacuum at 60 °C overnight.

Characterization

The powder x-ray diffraction (XRD) measurement was carried out on a Bruker D4 x-ray diffractometer (Germany). The scanning electron microscopy (SEM) images were taken on a Hitachi S-4800 microscope (Japan). The (HR)TEM images were acquired on a JEOL JEM-2011 transmission electron microscope (Japan) at 200 kV. The sample porosity was characterized by nitrogen sorption measurement at 77 K on a Micromeritics ASAP2020 apparatus. The specific surface area was determined based on the adsorption data using a Brunauer-Emmett-Teller (BET) method. The pore size distribution was determined from the adsorption branch of isotherms, and the total pore volume was figured out using the Barrett-Joyner-Halenda (BJH) model. The Pt content was measured by Inductively Coupled Plasma-Atomic Emission Spectrometry (ICP-AES) on a JA1100 Versa Probe spectrometer. X-ray photoelectron spectroscopy (XPS) measurement was conducted on a PHI 5000 Versa Probe system (Perkin Elmer) using monochromatic Al K α

radiation (1486.6 eV) operating at 25 W. All binding energies (BEs) were referenced to the C1s peak at 284.6 eV.

Electrochemical Measurement

A three-electrode cell system was used to perform all electrochemical tests. A Pt wire served as the counter electrode, a saturated calomel electrode (SCE) as the reference electrode, and a glassy-carbon (GC) disk (3 mm in diameter) decorated by catalysts as the working electrode. The working electrode was prepared as follows: catalyst powder of 2 mg was dispersed in a mixed solution of 700 μL water, 300 μL ethanol, and 30 μL Nafion (DuPont, 5 wt.%). After 1 h sonication treatment, a homogeneous black suspension was formed. Then, 10 μL suspension was dropped onto a GC electrode surface and dried at RT for 10 h. The potential was converted to the RHE scale based on the formula of $E_{\text{RHE}} = E_{\text{SCE}} + 0.244 + 0.059 \times \text{pH}$. Prior to the test, the electrolyte was bubbled with a N_2 flow for 30 min, and a continuous N_2 flow was supplied during the measurement to ensure continuous gas saturation. The electrochemical surface areas (ECSAs) of the catalysts were measured by the charge involved in the hydrogen adsorption/desorption region in a H_2SO_4 solution (0.5 mol L^{-1}) in cyclic voltammograms (CV). The electrocatalytic activity for EOR was examined by collecting CVs in a N_2 -purged H_2SO_4 solution (0.5 mol L^{-1}) and an ethanol solution (1 mol L^{-1}) at a scan rate of 50 mV s^{-1} . Several activation scans were performed until stable CV curves were obtained. In the CO stripping measurements, a monolayer of CO was adsorbed on the catalyst by flowing CO in a H_2SO_4 solution (0.5 mol L^{-1}) for 20 min while holding the electrode potential at -0.147 V . Non-adsorbed CO was removed by bubbling the electrolyte with a N_2 flow for 20 min. Stripping measurements were initiated from -0.2 to 1.0 V in the forward scan at 50 mV s^{-1} for at least two consecutive scans. The catalyst stability was measured by chronoamperometric (CP) test performed in a H_2SO_4 solution (0.5 mol L^{-1}) and an

ethanol solution (1 mol L⁻¹) at each potential for a period of 5000 s. All specific currents were normalized by the Pt mass determined by ICP-AES.

For product analysis, the electrocatalytic studies were conducted in an air-tight electrochemical cell. A piece of glassy carbon disk (1×1 cm²) was used as the working electrode, on which catalyst ink of 1 ml (2 mg/ml) was deposited. The electrolyte was a mixed H₂SO₄ (0.5 mol L⁻¹) and ethanol (1 mol L⁻¹) solution. The reaction products of ethanol electro-oxidation were determined and quantified by a gas chromatography (GC-122). A capillary column Plot-U (25 m of length and 0.32 mm of diameter) and a flame ionization detector (FID) were employed. The GC oven was programmed with the following temperature regime: initial temperature 33°C, hold for 6 min, ramp up to 130°C at 10°C/min [inlet (200°C) and detector (200°C)]. Mixtures of ethanol, acetaldehyde, and acetic acid were prepared for GC calibration. The chronoamperometric measurements were done at a constant potential of 0.65 V for a span of 7200 s and all the collected anodic aliquotes were cooled in an ice bath.

To analyze the products of EOR, additional electrocatalytic studies were conducted under potentiostatic conditions in an H-type electrochemical cell, in which the aliquots of the anodic effluent were collected at a maximum power density and analyzed by gas chromatography. The concentration of C₂H₅OH, CH₃CHO, and CH₃COOH were determined by using the standard curve method. The quantity of CO₂ is calculated based on the carbon balance from the consumption of ethanol subtracts the production of acetic acid and acetaldehyde.

The selectivity was calculated based on total amount of the reaction products from the anodic effluent,

$$\%S_p = \left(\frac{C_p}{\Delta C_{\text{ETOH}}} \right) \times 100\% \quad (1)$$

$$\%S_{\text{CO}_2} = 1 - \%S_{\text{AAL}} - \%S_{\text{AA}} \quad (2)$$

where C_p is the concentration of a specific reaction product (C_{AAL} = acetaldehyde, C_{AA} = acetic acid) and ΔC_{ETOH} is the change of ethanol concentration before and after reaction.

The turnover frequency (TOF) is a critical merit to reflect the inherent catalyst activity under the certain conditions. In the current study, the activities of the electrocatalysts are compared on the basis of the calculated TOF values. In other words, the converted ethanol molecules or the produced acetaldehyde/acetic acid/ CO_2 molecules on per surface Pt atom per second. The equations for TOF calculation are shown below:

$$TOF_{C_2H_5OH} = \frac{C_{C_2H_5OH} \times n_{C_2H_5OH}}{t \times \frac{\omega_{Pt} \times D_{Pt} \times m_{cat}}{M_{Pt}}} \quad (3)$$

$$TOF_i = \frac{C_{C_2H_5OH} \times n_{C_2H_5OH} \times Si}{t \times \frac{\omega_{Pt} \times D_{Pt} \times m_{cat}}{M_{Pt}}} \quad (4)$$

Where, $C_{C_2H_5OH}$ is the conversion of ethanol, $n_{C_2H_5OH}$ is the amount of ethanol added (in mol), t is the time scale, ω_{Pt} is the weight percentage of Pt in the catalyst, m_{cat} is the catalyst weight used, M_{Pt} is the molar mass of Pt, and D_{Pt} is the dispersion of Pt nanoparticles estimated by the mean particle size of Pt in terms of the statistical analysis of Pt particles in the HRTEM images. Si is the selectivity to the i product formed in the reaction.

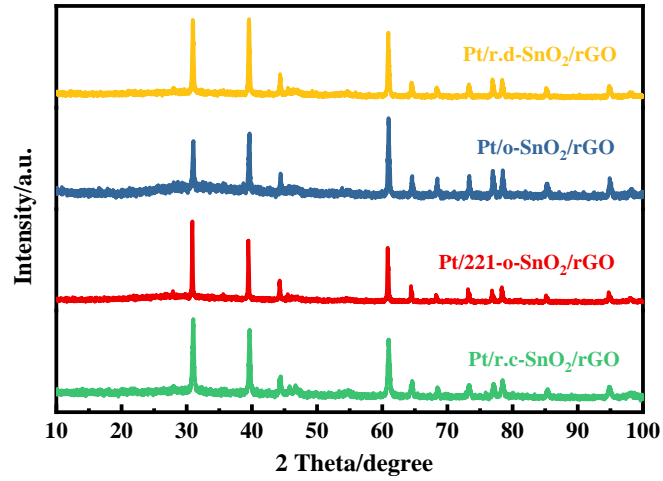


Fig. S1. XRD patterns of Pt/r.d-SnO₂/rGO, Pt/o-SnO₂/rGO, Pt/221-o-SnO₂/rGO, and Pt/r.c-SnO₂/rGO.

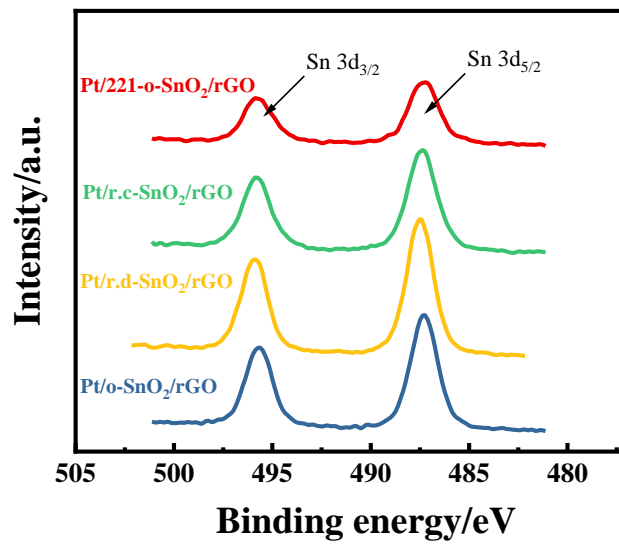


Fig. S2. Sn 3d XPS spectra of Pt/r.d-SnO₂/rGO, Pt/o-SnO₂/rGO, Pt/221-o-SnO₂/rGO, and Pt/r.c-SnO₂/rGO.

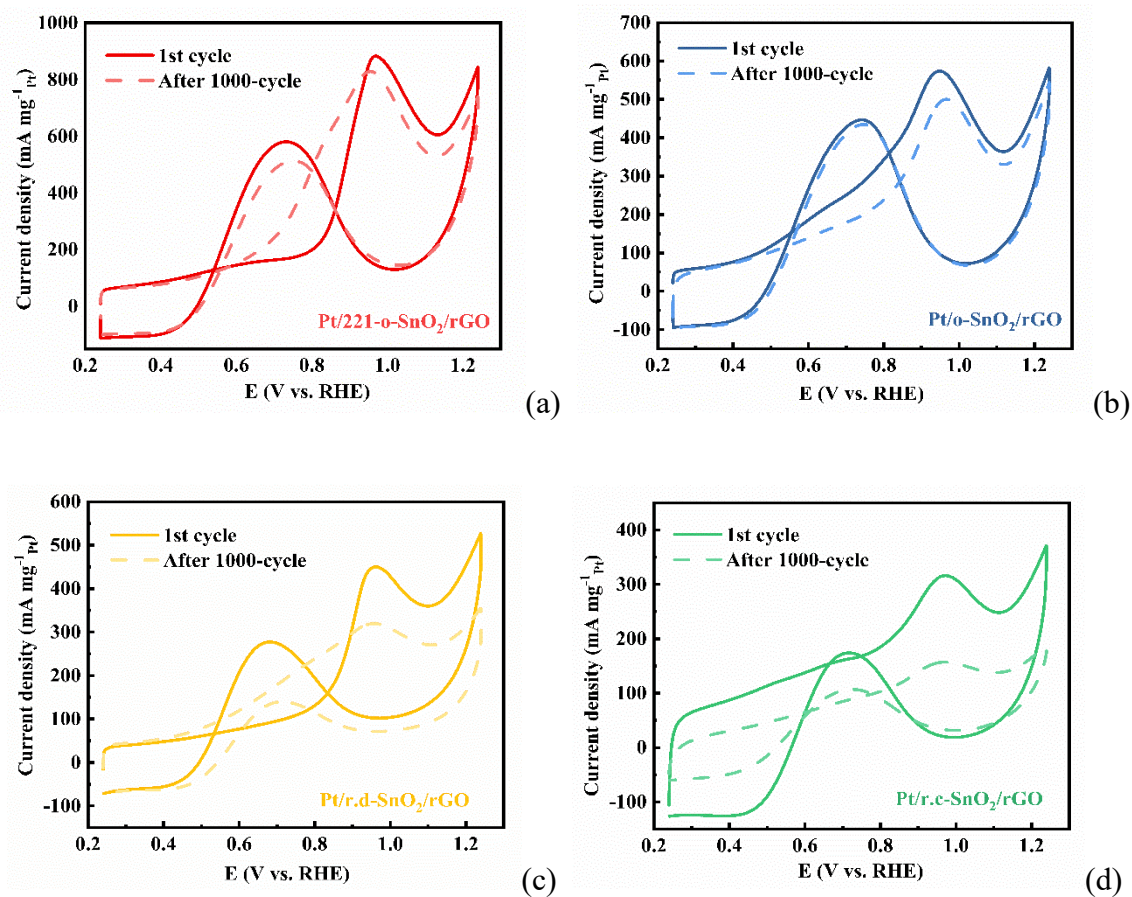


Fig. S3. Stability test over (a) Pt/221-o-SnO₂/rGO, (b) Pt/o-SnO₂/rGO, (c) Pt/r.d-SnO₂/rGO, and (d) Pt/r.c-SnO₂/rGO for the first cycle and after 1000-cycle at a scan rate of 100 mV·s⁻¹ in a solution of (0.5 M H₂SO₄ + 1.0 M C₂H₅OH).

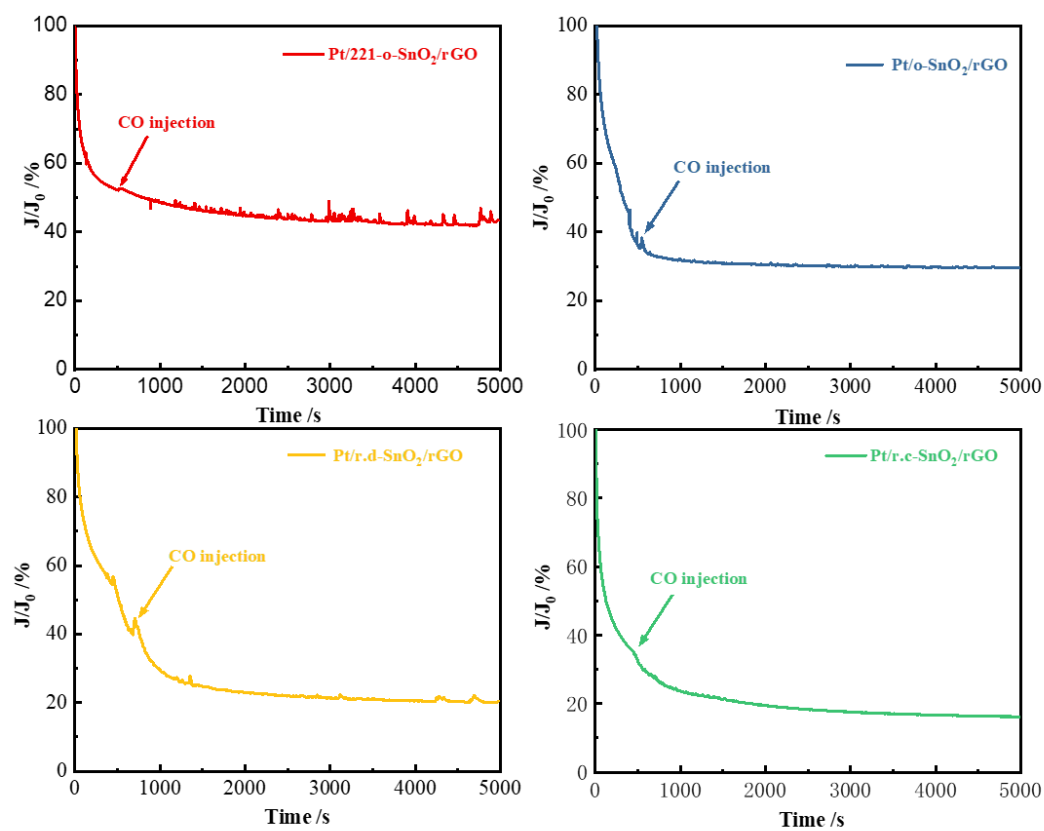


Fig. S4. Response of intentional CO poisoning. The dotted curves show the *i*-*t* relationships without the CO poisoning. Electrolyte: 0.5 mol L⁻¹ H₂SO₄ and 1 mol L⁻¹ ethanol.

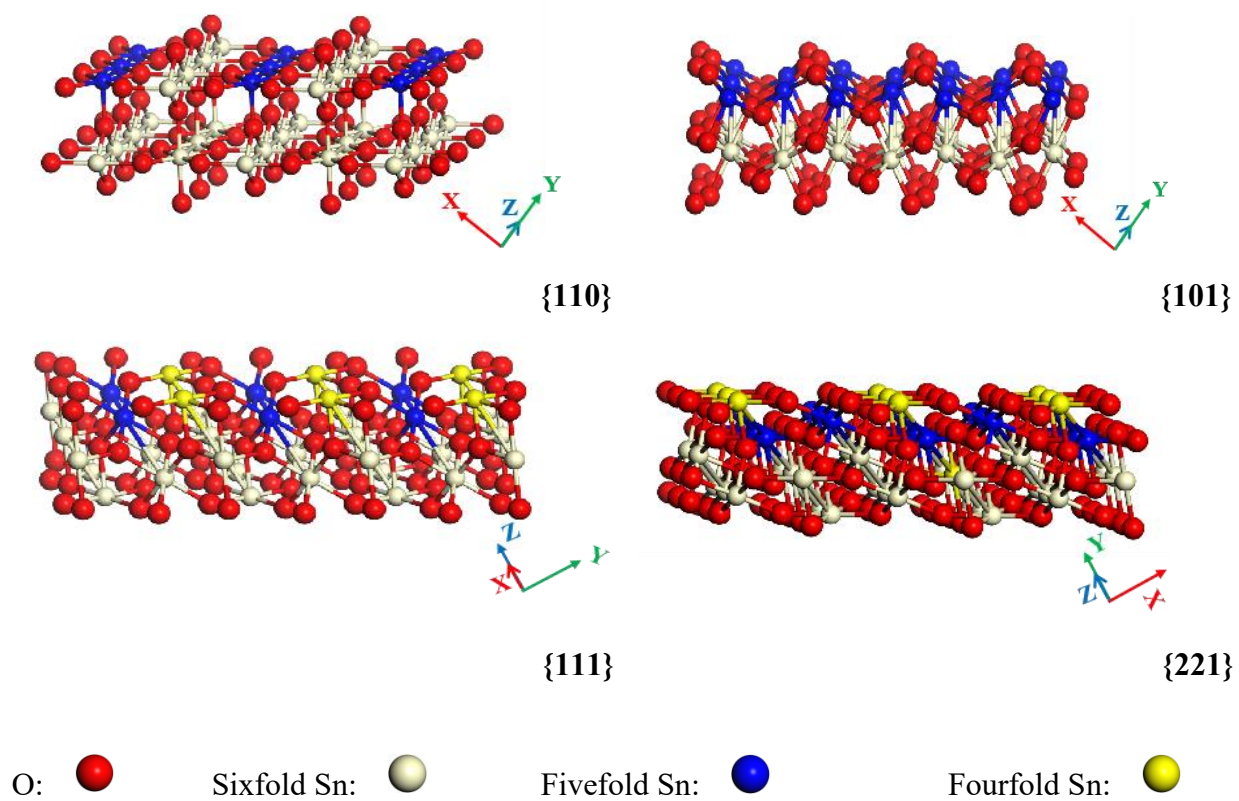


Fig. S5. Schematic illustrations of the un-reconstructed $\{110\}$, $\{101\}$, $\{111\}$, and $\{221\}$ facets of SnO_2 substrate.

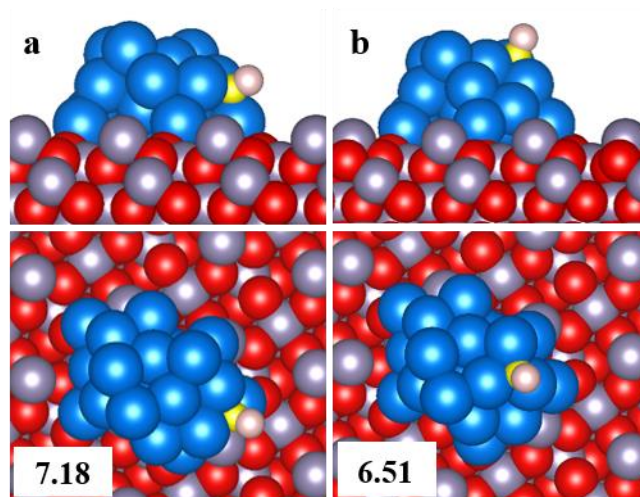


Fig. S6. The adsorption configuration of CH on Pt₂₁/SnO₂ (111). The red, purple, pink, blue, and yellow balls represent O atoms of SnO₂, Sn, H, Pt and C atoms, respectively. The indicated values are the adsorption energies (in eV) of the adsorbate on the corresponding substrates.

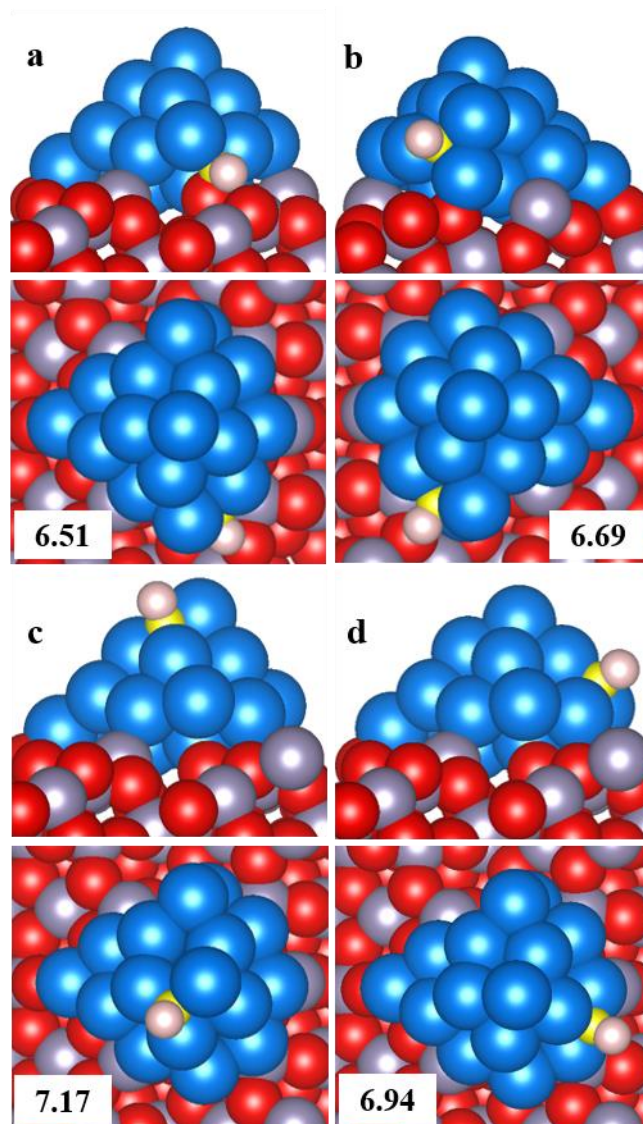


Fig. S7. The adsorption configuration of CH on Pt₂₁/SnO₂ (221). The red, purple, pink, blue, and yellow balls represent O atoms of SnO₂, Sn, H, Pt and C atoms, respectively. The indicated values are the adsorption energies (in eV) of the adsorbate on the corresponding interfaces.

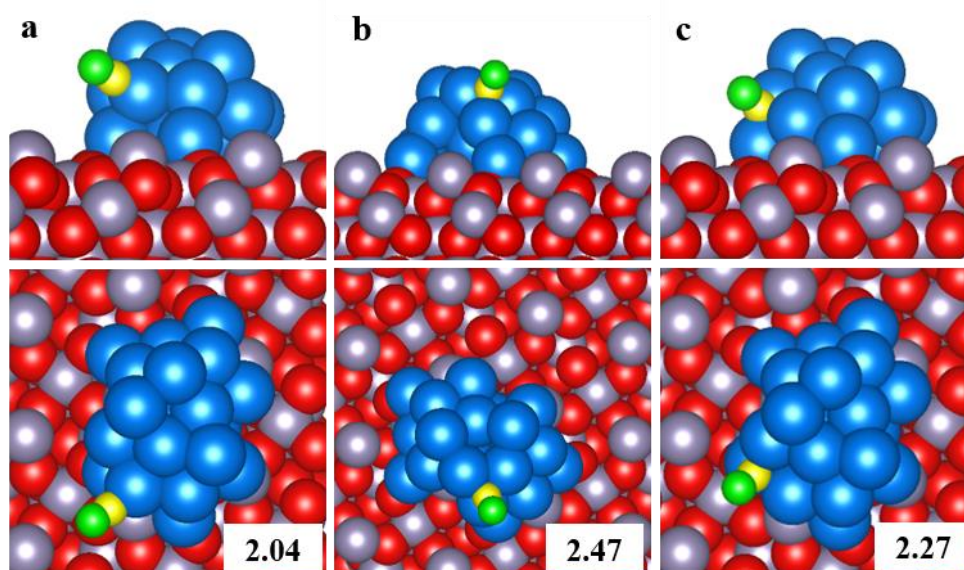


Fig. S8. The adsorption configuration of CO on Pt₂₁/SnO₂ (111). The red, purple, blue, and yellow balls represent O atoms of SnO₂, Sn, Pt and C atoms, respectively. The green balls represent O atom in CO. The indicated values are the adsorption energies (in eV) of the adsorbate on the corresponding interfaces.

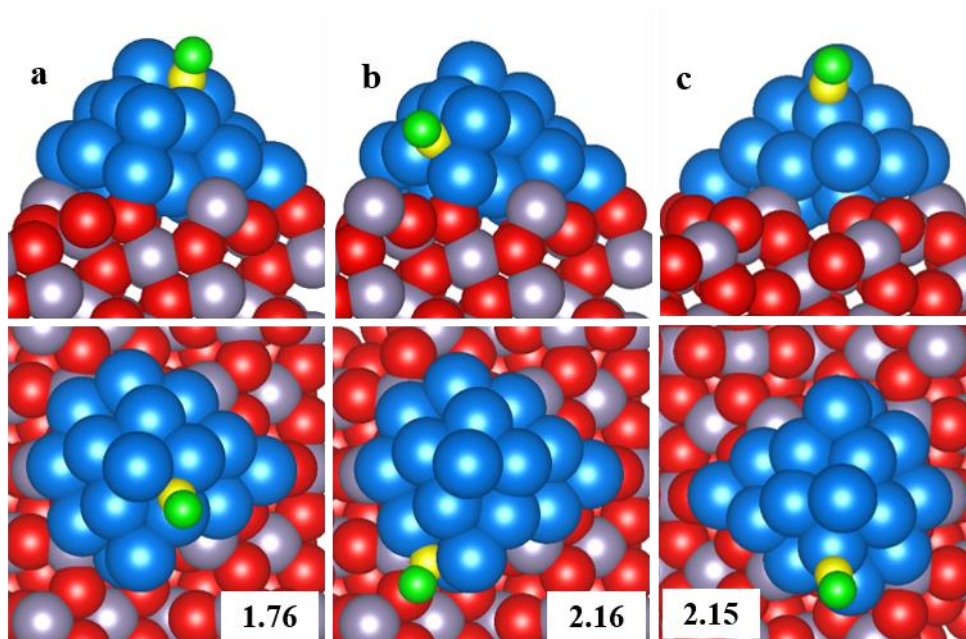


Fig. S9. The adsorption configuration of CO on Pt₂₁/SnO₂ (221). The red, purple, blue, and yellow balls represent O atoms of SnO₂, Sn, Pt and C atoms, respectively. The green balls represent O atom in CO. The indicated values are the adsorption energies (in eV) of the adsorbate on the corresponding interfaces.

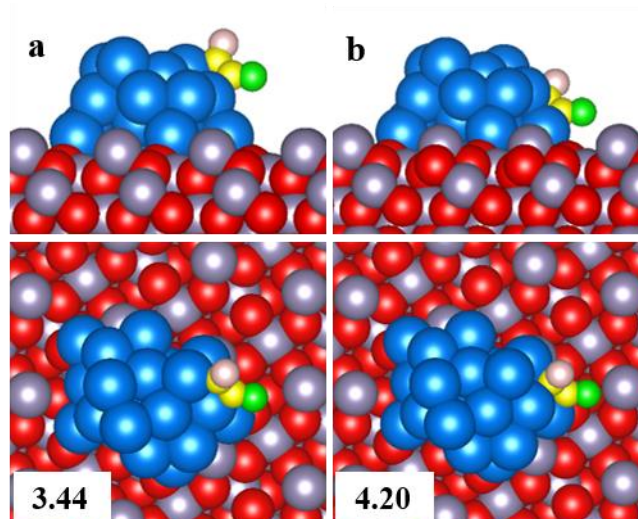


Fig. S10. The adsorption configuration of CHCO on Pt₂₁/SnO₂ (111). The red, purple, pink, blue, and yellow balls represent O atoms of SnO₂, Sn, H, Pt and C atoms, respectively. The green balls represent O atom in CHCO. The indicated values are the adsorption energies (in eV) of the adsorbate on the corresponding interfaces.

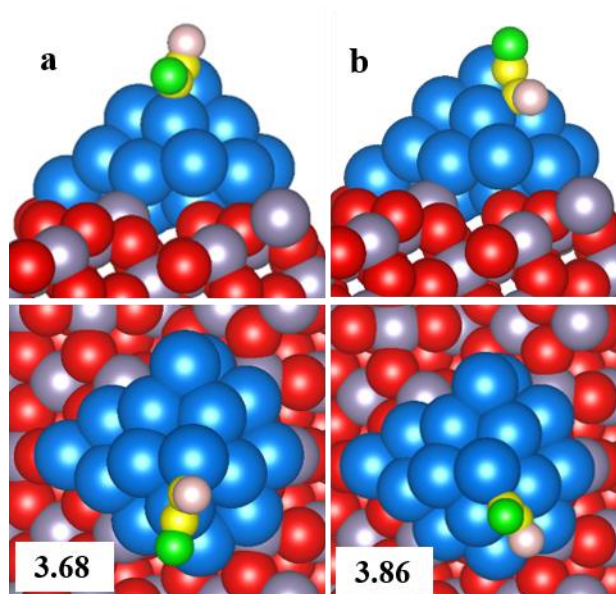


Fig. S11. The adsorption configuration of CHCO on Pt₂₁/SnO₂ (221). The red, purple, pink, blue, and yellow balls represent O atoms of SnO₂, Sn, H, Pt and C atoms, respectively. The green balls represent O atom in CHCO. The indicated values are the adsorption energies (in eV) of the adsorbate on the corresponding interfaces.

Table S1. Pt content measured by ICP-AES in various Pt/SnO₂ entities

Catalyst	Pt content (wt.%)
Pt/r.d-SnO ₂	8.9
Pt/o-SnO ₂	9.3
Pt/221-o-SnO ₂	9.1
Pt/r.c-SnO ₂	9.4

Table S2. EOR performance comparison over different catalysts

Catalyst	Substrate	Mass activity (mA mg ⁻¹ Pt)	Electrolyte	Onset Potential (V vs. RHE) from CO	Ref.
Au@Pt–Ru/SnO ₂	GCE	983.2	0.1 M HClO ₄ and 0.2 M ethanol	0.3	3
PtSn nanosheets	GCE	673.6	0.5 M H ₂ SO ₄ + 0.5 M EtOH	/	4
Pt-AuSnO _x	GCE	302	0.5 M H ₂ SO ₄ + 1 M EtOH	/	5
Rh@Pt _{3.5} L	GCE	809	0.1 M HClO ₄ and 0.2 M ethanol	/	6
Pt-Mo-Ni NWs	GCE	865.8	0.5 M H ₂ SO ₄ + 2.0 M EtOH	/	7
Rh@Pt CNCs/C	GCE	860	0.1 M HClO ₄ + 0.2 M EtOH	/	8
Pt ₃ Sn–SnO ₂ /NG	GCE	1365	0.5 M H ₂ SO ₄ + 1 M EtOH	0.33	9
Pt-0.5SnO _x /NCNC	GCE	1187	0.5 M H ₂ SO ₄ + 0.5 M EtOH	0.3	10
Pt/SnO ₂ /graphene	GCE	713	0.5 M H ₂ SO ₄ + 0.5 M EtOH	/	11
PtSn	GCE	774.1	0.5 M H ₂ SO ₄ + 1 M EtOH	/	12
Pt/211-o-SnO ₂ /rGO	GCE	1368.3	0.5 M H ₂ SO ₄ + 1 M EtOH	0.33	this work

REFERENCES

1. H.-F. Ma, T.-T. Chen, Y. Luo, F.-Y. Kong, D.-H. Fan, H.-L. Fang, W. Wang, *Microchimica Acta*. 2015, **182**, 2001-2007.
2. A. Mohammadi, N. Arsalani, A. Tabrizi, S. Moosavifard, Z. Naqshbandi, L. Ghadimi, *Chem. Eng. J.*, 2018, **334**, 66-80.
3. K. Siddharth, Z. L. Xing, F. Xiao, S. Q. Zhu, L. L. Zhang, F. Pan, M. H. Shao, *Chem-Asian J.*, 2020, **15**, 2174– 2180.
4. J. -Y. Chen, S. -C. Lim, C. -H. Kuo, H. -Y. Tuan, *J Colloid Inter. Sci.*, 2019, **545**, 54–62.
5. S. Dai, T. -H. Huang, P. -C. Chien, C. -A. Lin, C. -W. Liu, S. -W. Lee, J. -H. Wang, K. -W. Wang, X. Q. Pan, *J. Phys. Chem. Lett.*, 2020, **11**, 2846–2853
6. K. Liu, W. Wang, P. H. Guo, J. Y. Ye, Y. Y. Wang, P. T. Li, Z. X. Lyu, Y. S. Geng, M. C. Liu, S. F. Xie, *Adv. Func. Mater.*, 2019, **29**, 1806300.
7. J. J. Mao, W. X. Chen, D. S. He, J. W. Wan, J. J. Pei, J. C. Dong, Y. Wang, P. G. An, Z. Jin, W. Xing, H. L. Tang, Z. G. Zhuang, X. Liang, Y. Huang, G. Zhou, L. Y. Wang, D. S. Wang, Y. D. Li, *Sci. Adv.*, 2017, **3**, e1603068.
8. P. T. Li, K. Liu, J. Y. Ye, F. Xue, Y. Cheng, Z. X. Lyu, X. Y. Liao, W. Wang, Q. B. Zhang, X. J. Chen, M. C. Liu, S. F. Xie, *J. Mater. Chem. A*, 2019, **7**, 17987-17994
9. L. Wang, W. Wu, Z. Lei, T. Zeng, Y. Y. Tan, N. C. Cheng, X. L. Sun, *J. Mater. Chem. A*, 2020, **8**, 592–598
10. Z. Q. Zhang, Q. Wu, K. Mao, Y. G. Chen, L. Y. Du, Y. F. Bu, O. Zhuo, L. J. Yang, X. Z. Wang, Z. Hu, *ACS Catal.*, 2018, **8**, 8477-8483
11. Y. T. Qu, Y. Z. Gao, L. Wang, J. C. Rao, G. P. Yin, *Chem. Eur. J.*, 2016, **22**, 193-198.
12. F. X. Wu, D. T. Zhang, M. H. Peng, Z. H. Yu, X. Y. Wang, G. S. Guo, Y. G. Sun, *Angew. Chem. Int. Ed.*, 2016, **55**, 4952-4956.